AFRL-VA-WP-TR-2002-3006

AN INVESTIGATION OF THE AEROELEASTIC TAILORING FOR SMART STRUCTURE CONCEPTS

CINDY L. GIESE, GREGORY W. REICH,
MARK A. HOPKINS, AND KENNETH E. GRIFFIN

STRUCTURAL DESIGN & DEVELOPMENT BRANCH (AFRL/VASD)
2210 8TH ST.
B146 R301
WRIGHT-PATTERSON AIR FORCE BASE, OH 45433-7542

APRIL 1996

FINAL REPORT FOR PERIOD OF 23 AUGUST 1993 – 01 APRIL 1996

AIR VEHICLES DIRECTORATE
AIR FORCE RESEARCH LABORATORY
AIR FORCE MATERIEL COMMAND
WRIGHT-PATTERSON AIR FORCE BASE, OH 45433-7542

REPORT DOCUMENTATION PAGE

Form Approved
OMB No. 074-0188

1. AGENCY USE ONLY (Leave blank)	2. REPORT DATE	3. REPORT TYPE AND DATES COVERED
	April 1996	Final, 08/23/1993 – 04/01/1996

4. TITLE AND SUBTITLE

AN INVESTIGATION OF THE AEROELEASTIC TAILORING FOR SMART STRUCTURE CONCEPTS

5. FUNDING NUMBERS

C: In-House
PE: 62201F
PR: 2401
TA: SS
WU: 00

6. AUTHOR(S)

CINDY L. GIESE, GREGORY W. REICH, MARK A. HOPKINS, AND KENNETH E. GRIFFIN

7. PERFORMING ORGANIZATION NAME(S) AND ADDRESS(ES)

STRUCTURAL DESIGN & DEVELOPMENT BRANCH (AFRL/VASD)
2210 8TH ST.
B146 R301
WRIGHT-PATTERSON AIR FORCE BASE, OH 45433-7542

8. PERFORMING ORGANIZATION REPORT NUMBER

9. SPONSORING / MONITORING AGENCY NAME(S) AND ADDRESS(ES)

AIR VEHICLES DIRECTORATE
AIR FORCE RESEARCH LABORATORY
AIR FORCE MATERIEL COMMAND
WRIGHT-PATTERSON AIR FORCE BASE, OH 45433-7542
POC: Terry Harris, AFRL/VASD, (937) 255-8450

10. SPONSORING / MONITORING AGENCY REPORT NUMBER

AFRL-VA-WP-TR-2002-3006

11. SUPPLEMENTARY NOTES

12a. DISTRIBUTION / AVAILABILITY STATEMENT

Approved for public release; distribution unlimited.

12b. DISTRIBUTION CODE

13. ABSTRACT ***(Maximum 200 Words)***

This report describes a research effort demonstrating the concept of variable stiffness tailored aeroelasticity for smart structures. In particular, a wing structure is designed, or tailored aeroelastically, as a force multiplier for control actuation. This variable stiffness concept may be used as a way to employ light-weight and low-power output smart materials in lifting surface structures. A simple, unswept, rectangular wing model is used to explore the feasibility of utilizing the variable stiffness tailored structure as a force multiplier in conjunction with an outboard, trailing edge control surface. This approach involves the design of a simple wing model with adjustable stiffness to lower the control surface dynamic pressure and use the control surface as a "tab" to twist the wing.

14. SUBJECT TERMS

Smart Structures, Aeroelastic Tailoring, Control Actuation, Aeroelasticity, Variable Stiffness Concepts

15. NUMBER OF PAGES

14

16. PRICE CODE

17. SECURITY CLASSIFICATION OF REPORT	18. SECURITY CLASSIFICATION OF THIS PAGE	19. SECURITY CLASSIFICATION OF ABSTRACT	20. LIMITATION OF ABSTRACT
Unclassified	Unclassified	Unclassified	SAR

NSN 7540-01-280-5500

Standard Form 298 (Rev. 2-89)
Prescribed by ANSI Std. Z39-18
298-102

April 1996

AN INVESTIGATION OF THE AEROELASTIC TAILORING FOR SMART STRUCTURES CONCEPT

Cindy L. Giese,[1] Gregory W. Reich,[2] and Mark A. Hopkins[2]
Wright Laboratory
Wright-Patterson Air Force Base, Ohio

Kenneth E. Griffin[3]
Southwest Research Institute
San Antonio, Texas

Abstract

This paper describes an on-going research effort demonstrating the concept of variable stiffness tailored aeroelasticity for smart structures. In particular, a wing structure is designed, or tailored aeroelastically, as a force multiplier for control actuation. This variable stiffness concept may be used as a way to employ light-weight and low power output smart materials in lifting surface structures. A simple, unswept, rectangular wing model is used to explore the feasibility of utilizing the variable stiffness tailored structure as a force multiplier in conjunction with an outboard, trailing edge control surface. This experimental approach involves the design of a simple wing model with adjustable stiffness to lower the control surface reversal dynamic pressure and use the control surface as a "tab" to twist the wing. Analytical and experimental results are presented that indicate that it is possible to tailor the torsional stiffness of a wing such that the reversal speed is significantly reduced from a baseline stiffness configuration. The results of this study show where, for this example, use of the tailored structure as a force multiplier in conjunction with the trailing edge control surface may be beneficial.

I. Introduction

The application of Smart Structures technology offers some intriguing possibilities for high performance aircraft. Examples of applications of smart materials in aircraft structures include structural shape changes, flap deployment, and dynamic structural responses which may enhance an aircraft's lift production, reduce its aerodynamic drag and radar observability, and increase its structural health. These particular applications must be examined individually to determine the weight, size, power consumption, and power output requirements of the smart material for the specific intended task.

The Mission Adaptive Wing program in the 1980s was one of the first "smart," conformable wing programs. It examined the idea of smooth shape changes in flight to achieve improved performance for multiple flight conditions without conventional flaps. The program succeeded in demonstrating the benefits of this technology, however, the complexity and weight penalty of the conventional internal actuators prevented widespread implementation of the technology.

An entire body of research on Active Flexible Wing Technology demonstrated advantages of post-reversal aileron control utilizing multiple control surfaces on future aircraft designs. This approach did not require any heavy, complex actuators. The concept of tailored aeroelasticity for smart structures was inspired initially by this work.[1,2,3]

The research effort presented in this paper was conducted to explore experimentally the concept of aeroelastic tailoring of smart structures as presented by Griffin and Hopkins.[4] Their work documented the aeroelastic tailoring of an F-16 composite wing for smart structures materials applications. The wing was tailored to improve its ability to act as a force multiplier by decreasing the aileron reversal dynamic pressure enough to permit the aileron to be used in a post-reversal fashion for transonic maneuvering. The changes in reversal dynamic pressure are a result of adapting the structural stiffness of the primary structure as a function of the aircraft flight condition. The stiffness changes were performed to take advantage of the post-reversal aileron control using an outboard, trailing edge control surface.

---

[1]Aerospace Engineer

[2]Aerospace Engineer, Member AIAA

[3]Principal Engineer, Member AIAA

This investigation explores the feasibility of the concept defined in Reference 4 using a simple, unswept, rectangular wing, wind tunnel model. The model is designed so that the outboard, trailing edge control surface will reverse at two separate conditions within the envelope of a low speed wind tunnel. Two methods will be examined to change the spar stiffness and thus the reversal dynamic pressure: changing the length of the leaf springs that control pitch stiffness at the root, and replacing the baseline stiffness spar with a reduced stiffness spar. This paper presents the design of both of these methods and the results of a wind tunnel test which implemented the first method.

II. Wind Tunnel Model Design

The static aeroelastic phenomenon known as control surface reversal usually occurs at high dynamic pressure in aircraft with relatively flexible wings such as fighter aircraft. Near this flight condition, the effectiveness of the control surface is reduced substantially from that at much lower speeds due to wing twist under air load. Earlier research indicates the control forces created within this flight region may be improved if the control surface is permitted to reverse much earlier and operate in its post-reversal mode. A wind tunnel model was fabricated to examine this hypothesis

The following section describes the design of a "variable stiffness wing" wind tunnel model. The model is not representative of any existing aircraft wing design. Therefore, its mass and stiffness characteristics are not scaled to a particular vehicle. In order to simulate control force change due to a change in stiffness, the model must exhibit reversal in a low speed tunnel for both the baseline and reduced stiffness configurations. ASTROS and NASTRAN finite element analysis codes were used during the model design process to achieve the desired wind tunnel responses.

The wing model is thirty inches in span and eighteen inches in chord. It has a single spar, no sweep or taper, and a NACA 0012 airfoil section. In order to permit shape changes due to aeroelastic response, the wing aerodynamic shape is constructed using individual rigid wing sections with the span evenly divided into 6 sections. It has one outboard, trailing edge control surface spanning one wing section (LE at 75 percent chord). The single spar, extending over the entire length of the wing, is located at the wing quarter-chord. Each wing section is attached to the spar at the center of each section. The aileron structure has a small spar located near its leading edge, and is attached to the main outboard section with a rigid actuator and a hinge. Figure 1 is a general drawing of the wing, showing the main spar, aileron spar, wing sections, and the aileron.

Each wing section is made of two thin aluminum sheets, separated by foam, and covered on the outside with balsa. (Table 1 lists the material properties.) The sheets contain cutouts to reduce their mass, while retaining most of the chordwise stiffness required to maintain their shape. The sheets are riveted together and polyurethane foam is poured into the cavity between the sheets and allowed to harden. A side view of one of the sections is shown in Figure 2. Balsa is glued to the outside of the plates and shaped to a NACA 0012 airfoil. A thin layer of fiberglass is applied to the outside of the balsa to protect the surface of the model. Finally, lead weights are located in the front of each section to mass balance them about the quarter chord spar. The aileron is constructed of a solid piece of balsa that is reinforced with chordwise aluminum stiffeners.

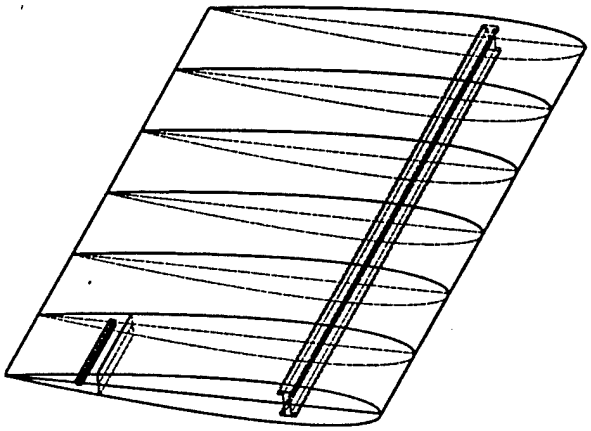

Figure 1. Assembled Wind Tunnel Model.

Table 1. Raw Material Properties.

Property	Aluminum	Foam	Balsa
Weight Density (lb/in.^{3})	0.101	0.00179	0.0023
Modulus of Elasticity (lb/in.^{2})	10.6×10^6	9950	7808
Shear Modulus (lb/in.^{2})	4.06×10^6	2700	1.93×10^4

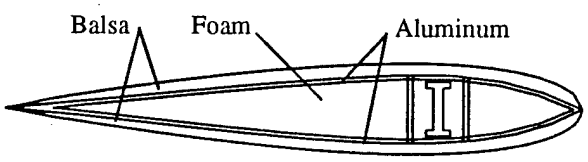

Figure 2. Side View of Wing Section.

The spar slides through the clearance hole in each section, and the sheets within each section are bolted to the spar at a single location. Attachment pads between

the spar and the plates help isolate the wing section stiffness from that of the spar. There is a 0.125 inch clearance between each section so that the sections are free to move independently of one another. These "gaps" are filled with foam rubber to keep air from flowing between the upper and lower surfaces of the model.

Two main spars are fabricated: one representing a baseline stiffness and the other a reduced torsional stiffness (see Table 2). The baseline stiffness spar is designed so that the control surface reverses near the upper limit of the wind tunnel's dynamic pressure range. The reduced stiffness spar is designed so the control surface reverses at approximately one half of the baseline stiffness spar's reversal dynamic pressure.

Table 2. Predicted Spar Properties.

Property	Baseline	Reduced
cross-sectional area (in.^{2})	0.5350	0.44000
I_1 (in.^{4})	0.10065	0.09273
I_2 (in.^{4})	0.01303	0.01138
J (in.^{4})	0.00954	0.00438
weight per unit length (lb/in.)	0.05404	0.04444
extra mass (lb/in.)	-	9.595e-3

The interchangeable main spars are both straight, untapered I-beams of similar size, fabricated of aluminum. Both have an overall height of 1.30 inches and an overall width of 0.75 inches. The top and bottom flanges on each spar are 0.15 inches thick. The baseline spar has a shear web thickness of 0.31 inches, while the reduced stiffness spar has a shear web thickness of 0.215 inches. In order to maintain the same mass distribution between the two spars, extra mass is added along the length of the reduced stiffness spar. The twelve attachment pads (6 top, 6 bottom) are machined as part of the spar. The dimensions of each of the pads are 1.25 x 0.50 x 0.07 inches.

The aileron spar is 0.25 inches square and is centered 0.50 inches behind the aileron hinge. The aileron hinge is located at the 75 percent chord location of the outboard section.

The assembled wind tunnel model is attached to a splitter plate which is in turn attached to the tunnel wall. The splitter plate elevates the model so that the boundary layer along the tunnel wall does not impinge on the model. The attachment between the splitter plate and the model allows for adjustments in the rigid angle of attack of the overall model, and in the torsional stiffness between the spar and the splitter plate mounting assembly. This attachment consists of two leaf springs and two bearings mounted on an L-bracket that is fixed to the splitter plate (Figure 3). The bearings are placed four inches apart and prevent translation of the spar but allow rotation about the centroid of the spar. The leaf springs provide variability of the torsional stiffness of the wing root by resisting rotation of the spar at its root. One end of each leaf spring is attached to the spar and the other is clamped to the L-bracket. The effective length of the leaf springs can be changed by varying the location of the clamp. This attachment allows investigation of variable stiffness in the wing root boundary conditions.

III. Preliminary Analysis

A simple finite element model was used to design the wind tunnel model using ASTROS and NASTRAN. Analyses performed include static load analysis for stress calculations on the spars, dynamic modal analysis, unsteady and steady aeroelastic responses (trim/reversal and flutter/divergence). All analyses were conducted at M = 0.20, at approximately 750 ft altitude (ρ = 0.002309 slug/ft^3) assuming standard conditions.

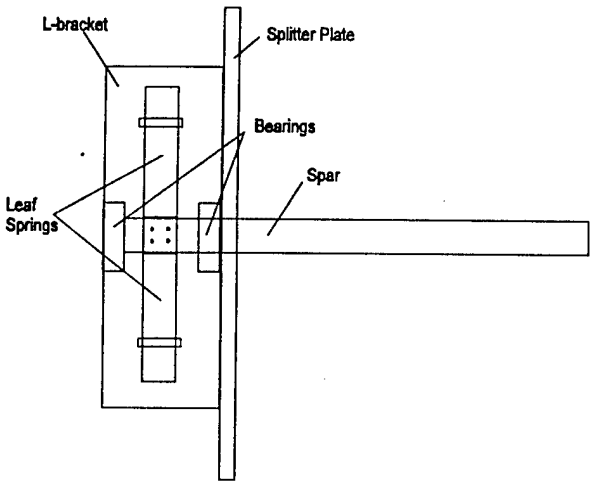

Figure 3. Top View of Spar Attachment.

During the design phase, the values for torsional stiffness of the spars were based on the equation for torsional stiffness of open-sectioned line elements, assuming no out-of-plane warping:[5]

$$J = \sum \beta_i b_i t_i^3$$

where b_i is the width of each flange, t_i is the thickness, and β_i depends on the ratio between the two. Bending stiffnesses used for model design were calculated based on the physical cross section of the spar. The finite element analyses of the wind tunnel model assumed stiffness was only contributed by the spar.

After fabrication of the model structural hardware, a static load analysis was conducted to ensure that the spar would not become over-stressed at some unaligned aerodynamic condition. The stresses in the analytical model were examined for the model at a constant 3° angle of attack in 80 psf flow, which is the upper dynamic pressure limit for the test. Steady lift loads were calculated for each section and applied at the quarter-chord of the section, the section to spar attachment location. The maximum root stress found for the baseline model was 8.661 x 10^3 psi and for the reduced stiffness model was 7.231 x 10^3 psi. Yield stress for 2024 T4 aluminum is 46 x 10^3 psi which results in a factor of safety of 5.31.

Dynamic modal analysis provided the basis for the unsteady aeroelastic analysis and also helped validate the finite element model. The baseline and reduced stiffness spar models demonstrated expected differences in vibration characteristics. Note, in Table 3, the first three out-of-plane modes are respectively wing root torsion (Figure 4), first wing bending (Figure 5), and first spar torsion (Figure 6). This first torsion mode is predominantly dependent on the pitch springs and the second torsion mode is predominantly dependent on the torsional stiffness of the spar.

Table 3. Comparison of Predicted Normal Modes (not mass-balanced, leaf spring 2 inches).

Baseline Spar		Reduced Spar		
Mode	Frequency (Hz)	Mode	Frequency (Hz)	Percent Difference
1 (T)	9.23	1 (T)	6.55	-29.04
2 (B)	18.14	2 (B)	17.08	-5.84
3 (T)	27.81	3 (T)	23.17	-16.68

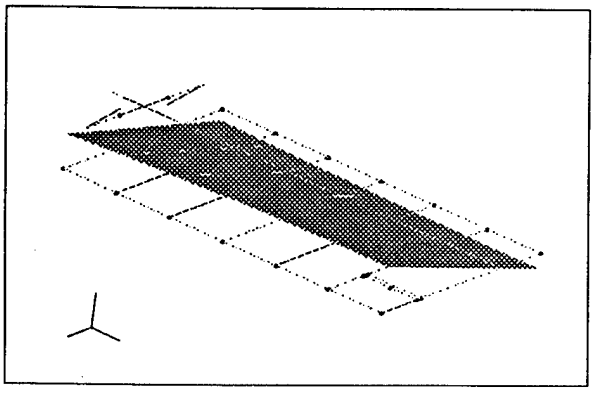

Figure 4. Wing Root Torsion Mode.

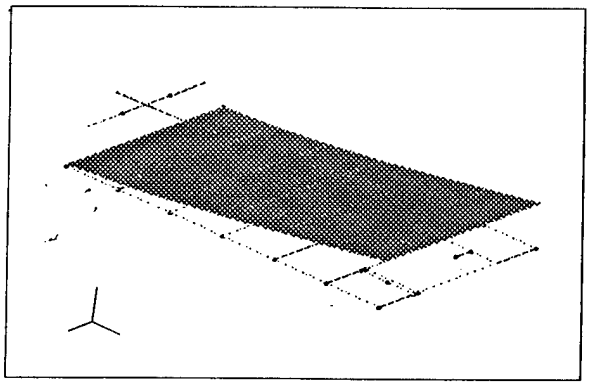

Figure 5. First Bending Mode.

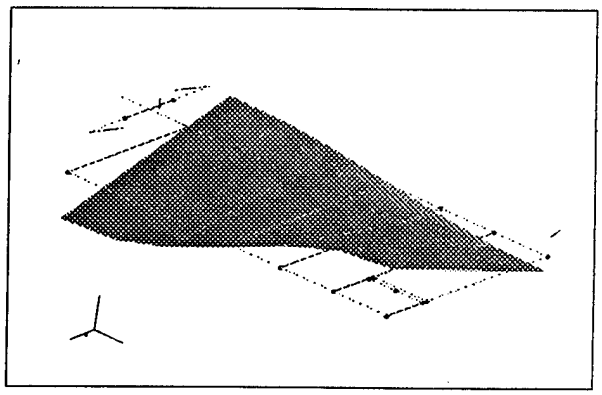

Figure 6. Second Torsion Mode (Spar Dependent).

The unsteady aeroelastic analysis was conducted to ensure the model would not undergo any aeroelastic instabilities within the tunnel envelope. Initial analyses using the calculated stiffnesses in Table 2 did not predict a flutter dynamic pressure within the tunnel envelope.

A closed-form steady aerodynamic analysis was performed using NASTRAN[6] to predict the conditions under which divergence may occur. Results indicted divergence above 620 psf for all model configurations, well outside of the tunnel envelope.

The steady aeroelastic analysis, performed using NASTRAN, calculated the simulated aircraft roll rate due to a known model of the aileron control surface deflection. The dynamic pressure was increased until the roll rate became negative for a constant Mach number. The trend predicted for the reduced and baseline spars is similar to the diagram in Figure 7 where the solid line represents the baseline stiffness configuration and the dashed line represents the reduced stiffness configuration. If the magnitude of the rolling moment for the reduced stiffness spar is multiplied by -1, the benefits of this force amplifier system can be visualized. The dynamic pressure at which the rolling

moment is zero is the reversal dynamic pressure. The dynamic pressure at which the rolling moment of the baseline stiffness spar is equal to the negative of the rolling moment for the reduced stiffness spar is called the critical dynamic pressure, q_{cr}. Above q_{cr}, the rolling moment of the wing is greater if the wing is allowed to employ the reduced torsional stiffness spar and use the flap in an aeroelastically reversed mode. The preliminary analysis using the calculated stiffness values in Table 2 predicted reversal of the baseline spar at 71 psf (248.0 ft/sec), while the reduced spar model reversed at 33 psf (169.1 ft/sec).

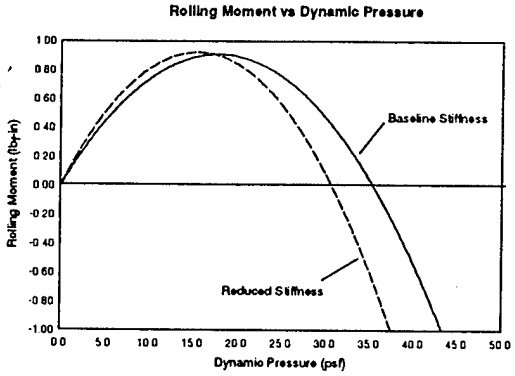

Figure 7. Rolling Moment Versus Dynamic Pressure.

IV. Hardware Testing

To date, the baseline spar and airfoil sections have been fabricated and tested. Manufacturing and testing of the reduced stiffness spar will be accomplished later this year. Stiffness properties of the baseline spar, mass moments of inertia of the wing sections, center of gravity locations of the wing sections, and vibrational frequencies of the assembled model have been experimentally determined. This section compares the experimental results and the predicted values employed in the model design phase.

Load Deflection Stiffness Tests

Stiffness measurements of the baseline spar were taken to verify the design stiffnesses. The procedure employed is outlined in Reference 7 and involved measuring rotational displacements through light reflection. Stiffness tests were accomplished with wing sections both "on" and "off" the spar, and the results are summarized in Table 4.

Table 4. Stiffness Values for Baseline Spar.

Property	Predicted	Sections Off	Sections On
I_1 (in.^{4})	0.10065	0.1005	0.1036
I_2 (in.^{4})	0.01303	0.0143	0.0158
J (in.^{4})	0.00954	0.00935	0.0130

The relatively large difference between the stiffnesses with the sections on and off can be attributed to the aluminum box formed by the aluminum sheets through which the spar is inserted (Figure 2). This box essentially closes the I-beam section and greatly stiffens the model, especially in torsion (27 percent increase in J).

Mass Moments of Inertia

The mass moments of inertia of each of the sections were experimentally determined and compared to predicted results from a three-dimensional computer model. The mass moments of inertia were obtained through a Bifilar pendulum swing test.[7] Results for the inboard five sections are summarized in Table 5, and those for the outboard section are in Table 6. The largest difference between the predicted and experimental values is in the aileron weight and its mass moments of inertia. This difference is due to a model change: the aileron was constructed of balsa wood with aluminum chordwise stiffeners instead of the aluminum and foam composite design similar to the wing sections as originally proposed.

Table 5. Comparison of Sectional Mass Moments of Inertia (mass-balanced sections).

Component	I (roll) lbm-in^2	I (pitch) lbm-in^2	I (yaw) lbm-in^2	Mass (lb)
Predicted Section 1-5	4.711	39.80	43.92	1.999
Section 1	5.616	48.01	51.92	1.994
Section 2	4.548	45.21	48.47	1.926
Section 3	4.493	44.96	48.49	1.924
Section 4	4.426	45.23	48.90	1.896
Section 5	4.500	41.91	45.33	1.916

Table 6. Comparison of Sectional Mass Moments of Inertia for Outboard Section.

Component	I (roll) lbm-in^2	I (pitch) lbm-in^2	I (yaw) lbm-in^2	Mass (lb)
Predicted Section 6	2.543	15.48	17.44	1.730
Section 6	2.285	14.45	14.75	0.879
Predicted Aileron	0.517	0.692	1.183	0.2477
Aileron	0.258	0.190	0.413	0.1013

The stiffness and mass moments of inertia values in the finite element model were updated with the experimental values once they were measured and validated. The results of the modal and aeroelastic analyses were updated using this semi-empirical model.

Ground Vibration Tests

Ground vibration tests were performed to compare predicted vibration frequencies to actual structure dynamics. As stated before, this comparison is

especially critical for the unsteady aerodynamics analysis to predict flutter. The vibration frequencies were obtained using a modal hammer and two accelerometers located in the outboard section of the model. Data in Tables 7 and 8 are the ground vibration test results for the 0.625 inch and 2.00 inch leaf spring length configurations. Other leaf spring length configurations yielded similar results. The predicted frequencies were determined using the experimental mass moments of inertia (Tables 5 and 6) and the sections "on" experimental stiffness values for the spar (Table 4).

Table 7. GVT and Predicted Vibration Frequencies (0.625" leaf spring, mass-balanced sections).

Mode	Predicted (Hz)	Test (Hz)	Percent Difference
1 (T)	12.39	12.34	0.405
2 (B)	18.00	16.00	12.50
3 (T)	37.00	37.82	2.17

Table 8. GVT and Predicted Vibration Frequencies (2.00" leaf spring, mass-balanced sections).

Mode	Predicted (Hz)	Test (Hz)	Percent Difference
1 (T)	9.79	8.89	10.2
2 (B)	17.12	15.21	12.6
3 (T)	31.07	30.0	3.57

Results from ASTROS and GVT compare very well with a leaf spring length of 0.625 inches for all modes except the first bending mode. The reason for this is suspected to be free play in the bearings and flexure in the L-bracket to which the spar is mounted behind the splitter plate. For a leaf spring setting of 2.00 inches, there is a larger difference between the analytical and experimental wing root torsion frequency. This suggests the finite element model of the flexible root boundary condition requires further refinement.

The flutter condition prediction was re-evaluated utilizing the experimentally measured spar stiffnesses and the mass moments of inertia. ASTROS indicated the model would flutter at 78 psf which is just within the tunnel envelope.

IV. Test Results

Flutter Encounter

The initial test configuration was the unmass-balanced model with the leaf springs clamped at their shortest length (0.625 inches). This model encountered flutter at 25 psf which was well below the predicted 78 psf. A re-evaluation of the flutter analysis revealed the importance of matching the first torsion and bending frequencies of the model. A much closer prediction of the actual flutter speed (28psf) was achieved when the stiffnesses of the spar were varied to match the analytical modal frequencies to the GVT bending and torsion frequencies. Since the flutter analysis is accomplished in the frequency domain, it was more important to match the analytical and experimental frequencies and mode shapes rather than the spar stiffnesses. The "tweaked" stiffnesses were only employed in the flutter calculation.

Further investigations of this model with ASTROS and TSO[8] revealed that if the center of gravity of each section was even slightly aft of the spar (the elastic axis location), then the model would be flutter prone at low dynamic pressures. These investigations also suggested that mass balancing all the airfoil sections about their spar attachments and reducing the torsional stiffness of the wing (using the leaf springs) would alleviate flutter within the tunnel envelope. Thus, the remaining test results are given for the mass-balanced model configuration.

Aeroelastic Tailoring

In order to test the control reversal effects of different wing root stiffnesses, data were taken for leaf spring lengths of 2, 3, and 4 inches over a dynamic pressure range of 0 to 80 psf. From Figure 8 it is apparent that variations of the torsional stiffness at the wing root generates large changes in the reversal dynamic pressure.

Further note in Figure 9 that the reversal dynamic pressure changed non-linearly with pitch spring length. This non-linearity may be the result of the rotation of the spar in the bearings (Figure 3). Note also that the amplitude in aileron deflection angle had very little effect on reversal dynamic pressure.

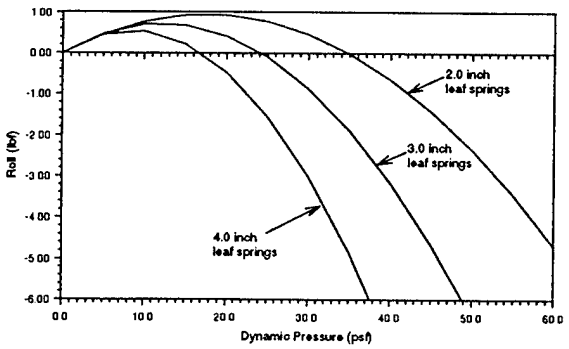

Figure 8. Roll Force Versus Dynamic Pressure for Leaf Spring Lengths of 2, 3, and 4 inches.

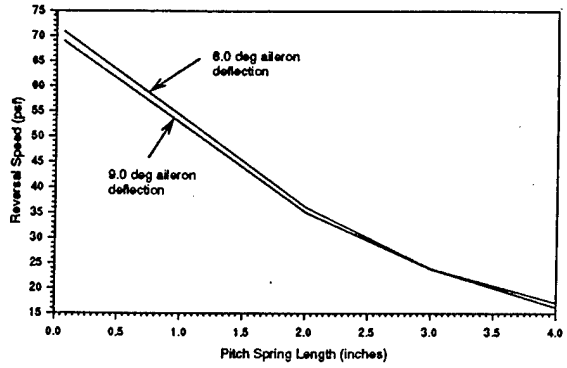

Figure 9. Reversal Dynamic Pressure Versus Pitch Spring Length

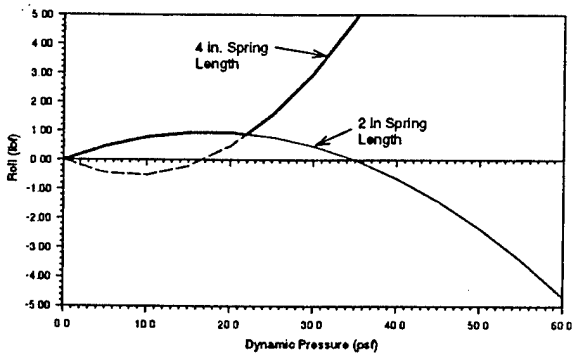

Figure 10. Roll Force Versus Dynamic Pressure for Simulated Stiffness Change

The advantages of variable stiffness aeroelastic tailoring are revealed by combining the best portion of the roll force versus dynamic pressure graph for the 2.0 inch leaf spring configuration with the negative of the 4.0 inch leaf spring configuration (Figure 10). The 2.0 inch leaf spring configuration represents a baseline stiffness which would be used in low-speed maneuvers. With increasing dynamic pressure the aileron effectiveness decreases and the "smart" wing stiffness is changed to its reduced stiffness configuration, represented by the 4.0 inch leaf spring. This switch allows the aircraft to utilize the increased roll authority available after roll reversal of the reduced stiffness spar by simply implementing a sign change in the control laws of the aircraft.

Reversal dynamic pressure predictions failed to accurately simulate the measured results. However, reconciliation of the differences has begun.

VI. Conclusions

This program begins the investigation of the feasibility and benefits of aeroelastic tailoring of smart structures using variable stiffness. A simple, rectangular wing demonstrated there are flight conditions where there is more roll authority available from a reduced torsional stiffness at the wing root than provided through aileron control using conventional stiffnesses. "Smart" wings that change stiffness can utilize this phenomena to extend flight envelopes and increase vehicle performance.

Further investigation is needed to compare effects of reducing spar stiffness as opposed to reducing the wing root stiffness. This will be addressed in the next wind tunnel entry later this year. The ultimate goal is to implement an active stiffness changing device in the wind tunnel model.

REFERENCES

1. Miller, G. D., "Active Flexible Wing (AFW) Technology," Air Force Wright Aeronautical Laboratory TR-87-3096, February 1988.

2. Pendleton, E., Lee, M., and Wasserman, L., "Application of Active Flexible Wing Technology to the Agile Falcon," Journal of Aircraft, Volume 29, May-June 1992.

3. Perry, B., III, Cole, S. R., and Miller, G. D., "A Summary of an AFW Program," Journal of Aircraft, Volume 32, January-February 1995.

4. Griffin, K. E. and Hopkins, M. A., "Aeroelastic Tailoring for Smart Structures," 36th Structures, Structural Dynamics, and Materials Conference, New Orleans, LA, 10-13 April 1995.

5. Venkayya, V. B., Tischler, V. A., and Bharatram, G., "NASTRAN Training Workshop," November 1994.

6. Rodden, W. P. and Johnson, E. H., MSC/NASTRAN: Aeroelastic Analysis User's Guide. Version 68. The Macneal-Schwendler Corporation. October 1994.

7. Pendleton, E., Lee, M., and Wasserman, L., "A Low Speed Flexible Model Simulating an F-16 Derivative Wing Design," Wright Research and Development Center, TR-90-3083, January 1991.

8. Lynch, R. W., et. al., "Aeroelastic Tailoring of Advanced Composite Structures for Military Aircraft," AFFDL-TR-76-100, February 1978.